

# Observation of a Membrane Fusion Intermediate Structure

Lin Yang<sup>1</sup> and Huey W. Huang<sup>2\*</sup>

We report the observation of a phase of phospholipid that contains a structure similar to the commonly postulated interbilayer state that is crucial to membrane fusion. The widely accepted model for membrane fusion suggests that there is an intermediate state in which the two contacting monolayers become continuous via an hourglass-shaped structure called a stalk. Many efforts have been made to estimate the free energy for such a state in order to understand the functionality of membrane fusion proteins and to define key parameters in energy estimates. The observation of the stalk structure supports the stalk hypothesis for membrane fusion and enables the measurement of these parameters experimentally.

confirm the existence of an exchange pathway between lysosomes (17, 20) and indicate that such movement occurs with rapid kinetics by a microtubule-dependent mechanism.

In summary, we have described a photoactivatable variant of GFP, PA-GFP, that provides a powerful tool for investigating fundamental questions in cell and developmental biology. Upon photoactivation, PA-GFP exhibits an optical enhancement of nearly two orders of magnitude under aerobic conditions, making it suitable to mark specific protein or cell populations. The speed with which an optical signal is obtained and the absence of signal from newly synthesized proteins, furthermore, make PA-GFP photoactivation a preferable labeling method to photobleaching for studying the temporal and spatial dynamics of proteins in vivo.

## References and Notes

- J. C. Politz, *Trends Cell Biol.* **9**, 284 (1999).
- H. Yokoe, T. Meyer, *Nature Biotechnol.* **14**, 1252 (1996).
- M. B. Elowitz, M. G. Surette, P.-E. Wolf, J. Stock, S. Leibler, *Curr. Biol.* **7**, 809 (1997).
- K. E. Sawin, P. Nurse, *Curr. Biol.* **7**, R606 (1997).
- J. S. Marchant, G. E. Stutzmann, M. A. Leissring, F. M. LaFerla, I. Parker, *Nature Biotechnol.* **19**, 645 (2001).
- M. Chalfie, Y. Tu, G. Euskirchen, W. W. Ward, D. C. Prasher, *Science* **263**, 802 (1994).
- R. Y. Tsien, *Annu. Rev. Biochem.* **67**, 509 (1998).
- Materials and methods are available as supporting material on Science Online.
- Supporting text is also available on Science online.
- K. Brejc *et al.*, *Proc. Natl. Acad. Sci. U.S.A.* **94**, 2306 (1997).
- G. J. Palm *et al.*, *Nature Struct. Biol.* **4**, 361 (1997).
- J. J. van Thor, T. Gensch, K. J. Hellingwerf, L. N. Johnson, *Nature Struct. Biol.* **9**, 37 (2002).
- R. Heim, D. C. Prasher, R. Y. Tsien, *Proc. Natl. Acad. Sci. U.S.A.* **91**, 12501 (1994).
- T. Ehrig, D. J. O'Kane, F. G. Prendergast, *FEBS Lett.* **367**, 163 (1995).
- J. Lippincott-Schwartz, E. Snapp, A. Kenworthy, *Nature Rev. Mol. Cell Biol.* **2**, 444 (2001).
- S. Kornfield, I. Mellman, *Annu. Rev. Cell Dev. Biol.* **5**, 483 (1989).
- Y. Deng, B. Storrie, *Proc. Natl. Acad. Sci. U.S.A.* **85**, 3860 (1988).
- V. Lewis *et al.*, *J. Cell Biol.* **100**, 1839 (1985).
- C. L. Howe *et al.*, *Proc. Natl. Acad. Sci. U.S.A.* **85**, 7577 (1988).
- A. L. Ferris, J. C. Brown, R. D. Park, B. Storrie, *J. Cell Biol.* **105**, 2703 (1987).
- We thank D. Piston (Vanderbilt University) for the pRSETA-wtGFP and pRSETA-EGFP plasmids and I. Mellman (Yale University) for the lgp120 cDNA. The monoclonal antibody, H4B4, developed by J. T. August and J. E. K. Hildreth was obtained from the Developmental Studies Hybridoma Bank developed under the auspices of the NICHD and maintained by the Department of Biological Sciences, the University of Iowa, Iowa City, IA 52242. We also thank N. Altan-Bonnet, I. Arias, J. Bonifacio, D. Hailey, K. Hirschberg, J. Hurley, C. Jackson, A. Pfeifer, E. Snapp, and T. Ward for critical readings of this manuscript. G.P. was an Intramural Research Training Award fellow during this work.

## Supporting Online Material

www.sciencemag.org/cgi/content/full/297/5588/1873/DC1

Materials and Methods

Supporting Text

Figs. S1 to S4

Tables S1 and S2

Movies S1 to S4

11 June 2002; accepted 5 August 2002

Membrane fusion takes place during many cellular processes, including membrane traffic, fertilization, and infection by enveloped viruses. Fusion allows the exchange of contents between different membrane compartments. In order to maintain the individuality of each of the intracellular compartments and of the cell itself, membranes do not fuse easily under normal circumstances. Thus, the process requires special proteins and is subject to selective control. Understanding the fusion mechanism is important not only for fundamental biology but also for medical applications such as drug delivery and gene therapy. Substantial progress has been made in the elucidation of the structures of membrane fusion proteins (1, 2) and in the estimations of the free energies for the rearrangement of lipid bilayers during fusion (3–8). Theoretical studies have identified the free energy barriers that suggest a requirement for mechanical work by fusion proteins, providing guidance for identifying the functions of protein structures. However, how proteins induce membrane fusion remains speculative, even in the best-studied case of viral fusion proteins (1, 9–13), because key intermediate structures have not been observed.

Membrane fusion between phospholipid bilayers can be induced by a variety of chemicals (14), perhaps most simply by multivalent ions (15, 16). The apparent role of multivalent ions is to bring two apposing lipid bilayers into contact. Here, we directly dehydrated the water layer between bilayers to achieve the same purpose. We started with a lipid spread on a flat substrate and exposed it to high humidity. Equilibrated under such conditions, the lipid formed a stack of parallel bilayers equally spaced by water layers (17).

When hydration was reduced, point contacts between bilayers occurred and the two apposed monolayers merged at the contact point and developed into an hourglass-like interbilayer structure (Fig. 1A) called a stalk (18, 19). This process is very likely analogous to the initial steps of membrane fusion. The difference here is that stalk structures were developed at numerous points of interbilayer contacts throughout the stack of bilayers. The system minimized energy by arranging the stalk structures into a regular lattice as in crystallization. This arrangement allowed us to inspect the stalk structure by x-ray diffraction.

One important characteristic of a lipid molecule is the ratio of the cross sections between its hydrophilic headgroup and its hydrocarbon chains. If this ratio is smaller than one, the lipid monolayer would have a tendency to bend toward the side of the headgroup. This is defined as a negative spontaneous curvature. It is well known that lipids with such a propensity tend to promote membrane fusion (20). We used diphytanoyl phosphatidylcholine (DPhPC), a lipid that has a negative spontaneous curvature. When DPhPC from organic solvent was deposited on a clean, flat substrate, it formed multiple parallel bilayers if the sample was kept warm (> 20°C) and in contact with saturated water vapor (21). To perform x-ray diffraction, we chose for the substrate a silicon nitride window (100 nm thick) spanned over a silicon frame, so that both transmissive and reflective diffraction could be recorded. Within the range of 20° to 30°C and relative humidity (RH) of 50 to 100%, three distinct diffraction patterns appeared (Fig. 1, B to E). Above ~80% RH, the lipid was in a lamellar ( $L_{\alpha}$ ) phase. The electron density profiles constructed from the diffraction patterns (Fig. 1C) showed that lipid bilayers, each ~3.8 nm in thickness, formed parallel lamella, intercalated with ~1-nm-thick water layers (22). When the relative humidity was decreased to between ~70 and ~80%, a different phase of phospholipid was discovered. The diffraction

<sup>1</sup>National Synchrotron Light Source, Brookhaven National Laboratory, Upton, NY 11973, USA. <sup>2</sup>Department of Physics and Astronomy, Rice University, Houston, TX 77251, USA.

\*To whom correspondence should be addressed. E-mail: hwhuang@rice.edu

## REPORTS

patterns in this phase (Fig. 1D) were consistent with unit cells arranged on a regular hexagonal lattice in each layer, similar to a layer of equal-sized spheres closely packed. For close-packed layers of spheres, there are two regular ways of stacking: the ABC stacking corresponding to the face-centered cubic lattice, or alternatively, the AB stacking corresponding to the hexagonal-closed packed lattice. The diffraction patterns of DPhPC correspond to ABC stacking (17), although they are not cubic, because the stacking distance is not geometrically related to the hexagonal lattice as in the case of closed-packed spheres. The symmetry of the new diffraction patterns is rhombohedral, space group  $R\bar{3}$ .

The three-dimensional electron density distribution was constructed from the complete diffraction pattern of the rhombohedral phase (23). To show the formation of a stalk structure, we took a hexagonal cylinder as unit cell from the midplane of a bilayer to the midplane of the next bilayer, with the cylindrical axis oriented normal to the plane of bilayers. At 28°C and 79% RH, the unit cell has a height of 4.43 nm, and each side of the hexagon is 3.95 nm. These dimensions vary slightly with temperature and humidity. In the  $L_\alpha$  phase, the unit cell consists of two planar monolayers separated by a water layer (Fig. 1C). But in the rhombohedral phase, the two apposed monolayers apparently merged and bent into an hourglass shape (Figs. 1D and 2). This is exactly what has been speculated as the stalk structure (3, 18). The direct observation of the stalk structure is important because there have been intense discussions as to what might be the free energy of such a structure (3–8).

When the degree of hydration was below  $\sim 70\%$  RH, the lipid showed a diffraction pattern (Fig. 1E) consistent with a two-dimensional hexagonal lattice (space group  $p6$ ). The electron density profiles (Fig. 1E) constructed from the diffraction patterns showed a hexagonal array of cylinders, in each of which a central water core was surrounded by lipid headgroups and the lipid chains extended diagonally outward. This pattern corresponds to an inverted hexagonal ( $H_{II}$ ) phase of lipids (24, 25). This phase of lipid has been observed previously in powdered forms in which polycrystals were randomly oriented. Here the lipid cylinders were all aligned parallel to the substrate. It has long been speculated that stalks are the intermediate state between the  $L_\alpha$  phase and the  $H_{II}$  phase (26). However, the stalk (rhombohedral) phase was not observed in previous studies of lamellar-to-inverted transitions (25). Apparently a direct transition between any two of the phases— $L_\alpha$ , stalk, and  $H_{II}$ —is possible.

The first major energy barrier for membrane fusion is closing of the distance be-

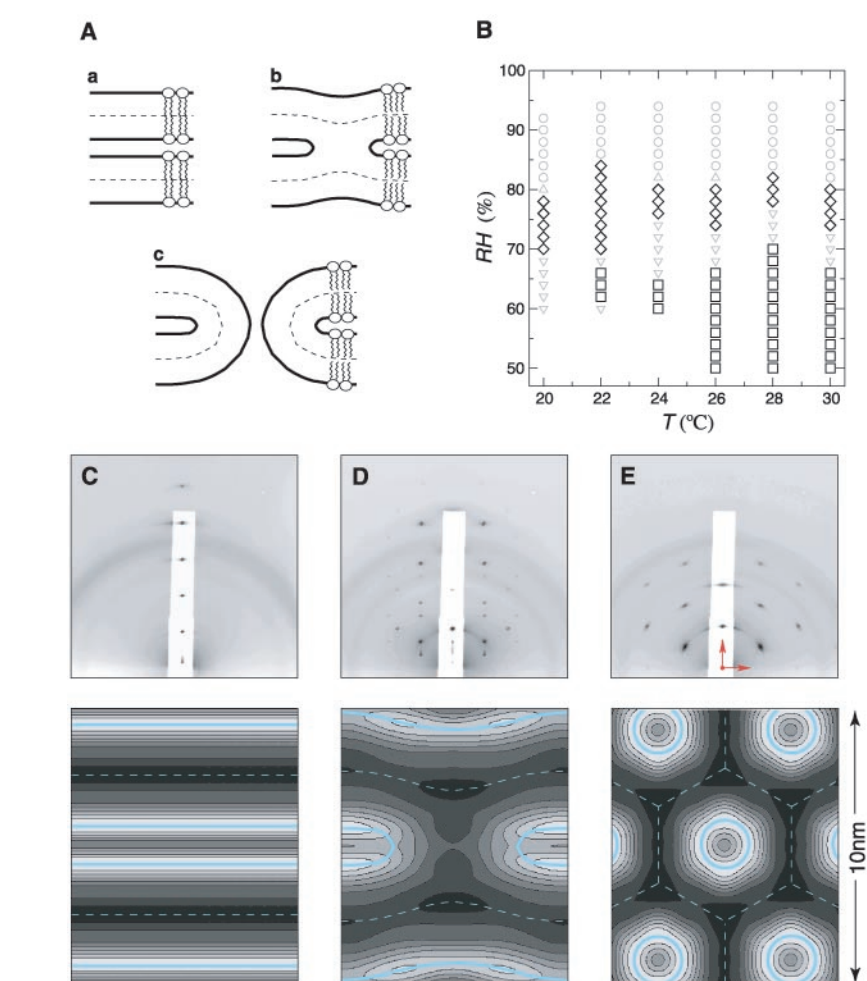


**Fig. 1.** (A) Schematics of lipid monolayer configurations undergoing membrane fusion. The prevailing theory of membrane fusion assumes that two apposed lipid bilayers (a) merge to an intermediate state called a stalk (b) and then form a fusion pore (c). (B) Phase diagram of lipid DPhPC as a function of temperature and hydration measured by the ambient relative humidity (RH). The symbols  $\circ$ ,  $\diamond$ , and  $\square$  correspond to the x-ray diffraction patterns shown in (C), (D), and (E), respectively. Symbols  $\Delta$  and  $\nabla$  indicate regions of coexistence. The x-ray diffraction patterns (C to E) were recorded on an area detector at a fixed incident angle such that the coordinates on the area detector were approximately in proportion to the reciprocal spacing. The ordinate, the  $z$  axis, is perpendicular to the substrate surface. The abscissa is proportional to the magnitude of the in-plane component of the reciprocal vector. (The crystalline domains were randomly oriented around the  $z$  axis.) All three patterns are on the same scale; high density is white and low density is black; blue lines indicate the regions of the highest (solid) and the lowest (dashed) densities; red arrows in (E) represent  $1.0 \text{ nm}^{-1}$  in the direction perpendicular and parallel to the substrate. (The white strip is the shadow of an x-ray attenuator.) (C) Diffraction pattern of a lamellar structure corresponding to the  $L_\alpha$  phase. The constructed electron density map shows aligned fluid bilayers parallel to the surface of the substrate, separated by water layers. (D) Diffraction pattern of a rhombohedral structure (space group  $R\bar{3}$ ). The constructed electron density map shows a stalk structure (see details in Fig. 2). (E) Diffraction pattern of a two-dimensional hexagonal structure (space group  $p6$ ) corresponding to the  $H_{II}$  phase. The constructed electron density map shows a hexagonal array of inverted lipid rods (perpendicular to the paper), each surrounding a water core.

tween two bilayers. This involves removing water between the two contacting surfaces. Experimentally this can be achieved by the introduction of multivalent ions (15, 16) or poly(ethylene glycol) (27), or by direct dehydration, as we did here. Once the two bilayers come into contact, a stalk structure forms. Within parallel multiple bilayers, the structure is stable, that is, in a state of minimum free energy. Theoretical studies concluded that there are two major contributions

to the free energy of a stalk structure: the energy associated with bending planar monolayers into the hourglass shape and the deformation and/or the void energy associated with the junctions of three monolayers (3–8). The estimates of energy depend on many assumed parameters, such as the size and shape of the stalk, the bending rigidity and spontaneous curvature of the lipid monolayer, and the composition of the lipid (whether it contains single or multiple components).

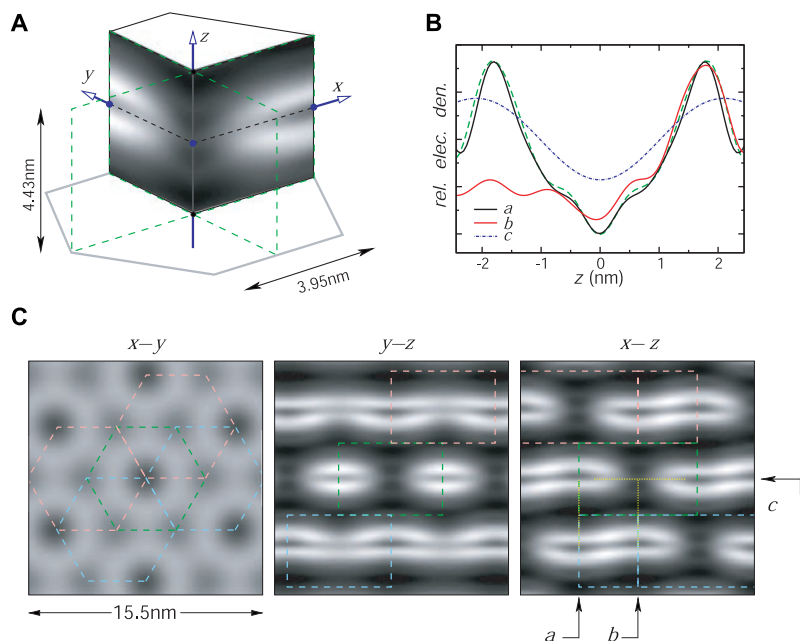


**Fig. 2.** Electron density distribution of the stalk structure. (High density is white, low density is black.) **(A)** A unit cell from the midplane of a bilayer to the midplane of the next bilayer in the  $z$  direction. The hourglass structure shows that two monolayers are merged (see also Fig. 1D). **(B)** Electron density profiles along the yellow lines  $a$ ,  $b$ ,  $c$  shown in the  $x$ - $z$  cut of **(C)**. For comparison, the green dashed line is the electron density profile across a bilayer from water layer to water layer in the  $L_{\alpha}$  phase. These are intended to show that the electron density distribution is consistent with a stalk structure as depicted in Fig. 1Ab. **(C)** Electron density maps on the  $x$ - $y$ ,  $y$ - $z$ , and  $x$ - $z$  planes, respectively, as defined in **(A)**. The green lines are the boundaries of the unit cell **(A)** in each plane. In the  $x$ - $y$  panel, the pink hexagons are two unit cells one layer above the green unit cell and the blue hexagons are one layer below. The boundaries of the pink and blue unit cells are shown as dashed rectangles in the  $y$ - $z$  cut and the  $x$ - $z$  cut.

The bending energy for a stalk structure is lowest at constant total curvature (7). From our low-resolution electron density profile (Fig. 1D), we can see that the contour of the highest density line (corresponding to the phosphate positions) is qualitatively consistent with the theoretical contour of constant total curvature predicted for a lipid of negative spontaneous curvature (7).

The main consequence of these results is the confirmation of the stalk hypothesis for membrane fusion. The stalk structure is indeed a natural consequence of two bilayers coming into contact, at least for the lipid DPhPC. To understand the functionality of

membrane fusion proteins, it is necessary to clarify the free energy pathway for the lipid conformation changes during fusion. The free energy of a stalk structure depends on its geometry and the properties of the lipid monolayer. The observation of the stalk structure in a stable phase can provide a way to experimentally measure these parameters and estimate its free energy of formation.

**References and Notes**

1. J. M. White, *Science* **258**, 917 (1992).
2. A. T. Brünger, *Curr. Opin. Struct. Biol.* **11**, 163 (2001).
3. D. P. Siegel, *Biophys. J.* **65**, 2124 (1993).
4. Y. A. Chizmadzhev, F. S. Cohen, A. Shcherbakov, J. Zimmerberg, *Biophys. J.* **69**, 2489 (1995).

5. P. I. Kuzmin, J. Zimmerberg, Y. A. Chizmadzhev, F. S. Cohen, *Proc. Natl. Acad. Sci. U.S.A.* **98**, 7235 (2001).
6. Y. Kozlovsky, M. M. Kozlov, *Biophys. J.* **82**, 882 (2002).
7. V. S. Markin, J. P. Albanesi, *Biophys. J.* **82**, 693 (2002).
8. B. R. Lentz, D. P. Siegel, V. Malinin, *Biophys. J.* **82**, 555 (2002).
9. R. W. Doms, *Methods Enzymol.* **221**, 61 (1993).
10. T. Stegmann, *Curr. Biol.* **4**, 551 (1994).
11. L. V. Chernomordik, E. Leikina, V. Frolov, P. Bronk, J. Zimmerberg, *J. Cell Biol.* **136**, 81 (1997).
12. T. Kanaseki, K. Kawasaki, M. Murata, Y. Ikeuchi, S. Ohnishi, *J. Cell Biol.* **137**, 1041 (1997).
13. B. R. Lentz, V. Malinin, M. E. Haque, K. Evans, *Curr. Opin. Struct. Biol.* **10**, 607 (2000).
14. A. E. Sowers, Ed., *Cell Fusion* (Plenum, New York, 1987).
15. J. Bentz, D. Alford, J. Cohen, N. Duzgunes, *Biophys. J.* **53**, 593 (1988).
16. H. Ellens *et al.*, *Biochemistry* **28**, 3692 (1989).
17. L. Yang, T. M. Weiss, R. I. Lehrer, H. W. Huang, *Biophys. J.* **79**, 2002 (2000).
18. D. Gingell, I. Ginsberg, in *Membrane Fusion*, G. Post, G. L. Nicholson, Eds. (Elsevier, Amsterdam, 1978), pp. 791–833.
19. V. S. Markin, M. M. Kozlov, V. L. Borovjagin, *Gen. Physiol. Biophys.* **3**, 361 (1984).
20. L. V. Chernomordik, M. M. Kozlov, J. Zimmerberg, *J. Membr. Biol.* **146**, 1 (1995).
21. The techniques for preparing aligned multilamellar bilayers were described by S. Ludtke, K. He, and H. W. Huang [*Biochemistry* **34**, 16764 (1995)].
22. W. C. Hung, F. Y. Chen, H. W. Huang, *Biochim. Biophys. Acta* **1467**, 198 (2000).
23. The phases of the diffraction amplitudes were determined by the swelling method as suggested by M. F. Perutz, *Proc. R. Soc. London Ser. A* **225**, 264 (1954). See text in supporting online material (SOM) for a description of the phasing procedures.
24. V. Luzzati, in *Biological Membranes*, D. Chapman, Ed. (Academic Press, New York, 1968), pp. 71–123.
25. D. C. Turner, S. M. Gruner, *Biochemistry* **31**, 1340 (1992).
26. D. P. Siegel, *Biophys. J.* **76**, 291 (1999).
27. S. W. Hui, T. L. Kuhl, Y. Q. Guo, J. Israelachvili, *Colloids Surf. B* **14**, 213 (1999).
28. We thank D. Siegel and W.-P. Su for valuable comments and W. A. Caliebe for experimental assistance. This work was supported by NIH grant GM55203 and by the Robert A. Welch Foundation. Research carried out in part at the beamline X21 of the National Synchrotron Light Source, Brookhaven National Laboratory, which is supported by the Department of Energy, Division of Materials Sciences and Division of Chemical Sciences, under contract no. DE-AC02-98CH10886.

**Supporting Online Material**

www.sciencemag.org/cgi/content/full/297/5588/1877/DC1  
 SOM Text  
 Figs. S1 and S2  
 Table S1

24 May 2002; accepted 29 July 2002